Spatial Domain Superresolution Reconstruction of Images

by

Kaushlendra Singh Sisodia

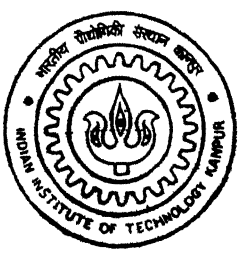

DEPARTMENT OF ELECTRICAL ENGINEERING

INDIAN INSTITUTE OF TECHNOLOGY, KANPUR

February, 2001

Spatial Domain Superresolution Reconstruction of Images

A Thesis Submitted
in Partial Fulfillment of the Requirements
for the Degree of
Master of Technology

by
Kaushlendra Singh Sisodia

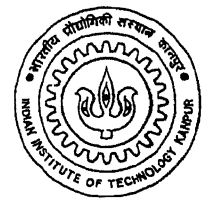

to the
Department of Electrical Engineering
Indian Institute of Technology, Kanpur

February, 2001

Certificate

This is to certify that the work contained in the thesis entitled "*Spatial Domain Superresolution Reconstruction of Images*", by *Kaushlendra Singh Sisodia*, has been carried out under our supervision and that this work has not been submitted elsewhere for the award of a degree.

(Dr. K. S. Venkatesh)
Deptt of Electrical Engineering,
Indian Institute of Technology,
Kanpur.

(Dr. Sumana Gupta)
Deptt of Electrical Engineering,
Indian Institute of Technology,
Kanpur.

Acknowledgement

I would like to thank to my thesis supervisors for their best guidance, advice, tolerance and continuous encouragement during the thesis work and more than anything else their faith in me. I will cherish my association with them for years to come. They have allowed me to learn and pursue various other interests of mine without any interference and I am very happy to have been their student.

I am indebted to my parents whose inspiration and upbringing could bring me to the portals of my present achievement. I am thankful to my friends especially Rajiv Bajpai, Amitava Mukherjee, Ashwani and Vinay, whose encouragement and continuous interaction lead me to successfully completion of my thesis.

Finally I am thankful to Almighty and my saviour Bhagvan, without his blessing and guidance nothing would have been possible.

Abstract

Superresolution (SR) reconstruction for a linear space variant point spread function (LSV PSF) is highly computationally intensive and generally ill conditioned. In this thesis we propose two algorithms for spatial domain reconstruction of SR images. The first algorithm includes recursive SR reconstruction of an image from several undersampled degraded frames, blurred by a space varying medium, with better reconstruction results than the existing method. The second algorithm includes a computationally efficient method for separable PSF taking the fact that 2-D shift matrix and 2-D downsampling matrix are always separable and for getting a stable and unique solution of the ill-conditioned equations we use empirical regularized least square method.

Synopsis

The superresolution(SR) reconstruction of a high resolution image is an image restoration method from several degraded low resolution frames The superresolution concept evolved because large telescopes have reached a limit of practical realization, restricted by the high costs of manufacturing large and precise optics. Superresolution overcame these limitations by processing low resolution images and reconstructing a high resolution image. The concept behind SR reconstruction is to extract different(extra) information from each degraded frame of low resolution frame and to use it to reconstruct a high resolution image.

Superresolution reconstruction for a linear space variant point spread function (LSV PSF) is highly computationally intensive and generally highly ill conditioned. The results in the thesis, motivated by the need to satisfactorily process different satellite pictures, are, however applicable in other situations which are faced with space variant blurring and noise addition. The algorithms and techniques outlined provide noise reduction and an increase in spatial resolution using several blurred images of a common object. In this thesis we propose two algorithms for spatial domain reconstruction of SR images. The first algorithm includes recursive SR reconstruction of an image from several undersampled degraded frames, blurred by a space varying medium, with better reconstruction results than the existing method. The algorithm may be used for reconstruction of an SR image from several frames obtained from multiple cameras with different sensor element sizes with each frame degraded by a different PSF. Computational complexity can be further reduced by using iterative methods.

The second algorithm includes a computationally efficient method for separable PSF taking the fact that 2-D shift matrix and 2-D downsampling matrix are always separable and for getting a stable and unique solution of the ill-conditioned equations we use empirical regularized least square method.

After each update of the estimate, we use the a priori information that each pixel value in the source image is nonnegative.

Contents

List of Figures

Chapter 1

Introduction

1.1 Introduction and motivation

Superresolution reconstruction is a method of image restoration. The field of image restoration began primarily with the efforts of scientists involved in the space programs of both the United States and the former Soviet Union in the 1950s and early 1960s. These programs were responsible for producing many incredible images of the earth and our solar system that were hitherto unimaginable. Such images held untold scientific benefits which only became clear in ensuing years as the race for the moon began to consume more and more of scientific effort and budgets. However, the images obtained from the various planetary missions of the time, such as the Ranger, Lunar Orbiter, and Mariner missions, were subject to much photographic degradation. This was the result of substandard imaging environments, the vibration in machinery and the spinning and tumbling of the space craft.

The superresolution concept evolved because large telescopes have reached a limit of practical realization, restricted by the high costs of manufacturing large and precise optics. Superresolution overcame these limitations by processing low resolution images and reconstructing a high resolution image.

Several Earth Resources Technology (ERTS) Satellites (renamed later as LANDSAT) were launched to obtain multispectral images for subsequent processing in order to identify different environment phenomenon such as the distribution and general type of vegetation, regional geological structures, and the area extent of surface water. Each LANDSAT flew in a circular orbit, about 570 miles above the surface of earth, executing circles approximately 14 times per day. Each daytime orbital pass was from north to south with repetitive coverage every 18 days or so.

The superresolution (SR) reconstruction principle as applied upon several frames came somewhat later, with the launch of the widely publicized Hubble Space Telescope. Launched in 1990 as a joint project of the North American and European space agencies NASA and ESA, this optical observatory was designed to yield a breakthrough in astronomy by providing space images with unprecedented spatial resolution. Unfortunately, soon after the launch, engineers discovered a manufacturing defect in the main mirror of the tele-

scope, leading to severe distortion that could eventually be fixed only in late 1993. The astronomers improved the blurred images obtained from the Hubble craft by numerical reconstruction, i.e., by solving an inverse problem.

The results of the thesis, motivated by the need to satisfactorily process different satellite pictures, are, however applicable in other situations which are faced with space variant blurring and noise addition. The algorithms and techniques outlined provide noise reduction and an increase in spatial resolution using several blurred images of a common object.

With the availability of frame grabbers capable of acquiring multiple frames of video, there is a growing interest in superresolution image reconstruction from video, as well as video reconstruction, whereby multiple frames are used to overcome the inherent resolution limitations of a low-resolution camera system. SR reconstruction proves useful in many practical applications, including printing SR stills from video, where it is desired to enlarge an image and increase the detail. Because video signals are commonly interlaced, creating SR stills requires a combination of deinterlacing and the removal of acquisition degradation.

1.2 Superresolution Reconstruction

The SR concept in image restoration as originally formulated around the 1970's has now undergone an evolution, and the present-day idea of SR reconstruction is somewhat different even though the basic concept remains the same:

An incoherent object scene $O(x)$ is a spatial radiance distribution; it therefore cannot be negative:

$$O(x) \geq 0, \ all \ x. \tag{1.1}$$

Let us consider the problem of restoring $O(x)$ from knowledge of its degraded image $I(y)$ and the point-impulse response $S(x)$ characteristic of the imagery.

Let the unknown object be an incoherent, planar radiance distribution. The object plane is imagined to be subdivided into J equal-sized, elemental cells of extent Δx, and x_j locates the center of the jth cell. (We use one-dimensional notation, for simplicity.) It is logical to make Δx just the required limit of resolution desired by the user in the final restoration. It therefore suffices to represent the object as a sequence of average radiance values $O(x_j) = O_j$, j=1,2, . . . , J, over the elemental cells. The light from an object is assumed to be imperfectly imaged by a linear system such as a lens. An image plane intercepts the light and the formed image is sampled by a sensor array at points $y(m)$; $m = 1, 2, 3, \ldots, M$. If the image is bandlimited, it obeys a sampling theorem. In this case it is natural to space the sensor points $y(m)$ uniformly at the Nyquist interval.

In order to permit a higher resolution in the restoration of $O(j)$ than in the image, object-cell size Δx must be smaller than the image-data interval,

$$\Delta x < y(m) - y(m-1) \tag{1.2}$$

This is the basic concept of superresolution. We can present the superresolution concept in either of the following two ways:

1.2.1 The Classical Concept

The original SR problem was posed as follows: can photographic images such as those of star clusters be superresolved? Can already good images be improved by a restoring method? To study the question, objects have been prepared that can be resolved only if the bandwidth in the restoration exceeds that of image data. Hence superresolution was known as extrapolation of the signal, that could be applied to a space limited function (i.e. $f(x) = 0\ for\ |x| > \alpha$) whose Fourier transform is given over a finite frequency band. Extrapolation of the spectrum of an object beyond the known frequency band of the imaging system is called Superresolution. The detected image I(y) of an incoherent object O(x) is formed through a linear relation:

$$I(y) = \int_{scene} O(x)S(y-x)dx + N(y) \tag{1.3}$$

where x, y are space coordinates and O, I have units of radiance and irradiance, respectively. N(y) is random noise that is characteristic of the particular method chosen for detecting the image. S(y) is the diffraction image of a point object, and is called the point spread function(psf).

Now the problem is inversion of (1.3) for restoration of object O(x), i.e., estimating O(x) when I(y) and S(y) are known at a given subdivision of points y, and to a given level of accuracy. We call the estimate of O(x) its restoration, and denote it as $\hat{O}(x)$.

Two main obstacles to perfect restoration of O(x) are the presence of noise N(y) in the image data, and a sharp cutoff in the spectrum s(ω) of the PSF. If we denote the cutoff frequency for s(ω) as Ω , Fourier inversion of (1.3) yields:

$$i(\omega) = o(\omega)s(\omega) + n(\omega) \qquad for\ |\omega| < \Omega \tag{1.4}$$

$$n(\omega) \qquad for\ |\omega| \geq \Omega \tag{1.5}$$

Lower case quantities in (1.4) and (1.5) correspond to the Fourier transform of the capitalized quantities in (1.3). Evidently, the existence of a finite Ω causes the image spectrum to lack components at all frequencies $|\omega| \geq \Omega$. This seems to apply that these higher - frequency components of the object cannot ever be recovered in the restored image. If so, the resolution in the restoration would be limited to a smallest separation of about

$$2 * pi/\Omega = R, \tag{1.6}$$

depending on the choice of resolution criterion that is used. R is called the Rayleigh resolution length.

1.2.2 The Modern View

During 1990's superresolution idea became somewhat changed now instead of single frame, many frames were used for reconstruction of a high resolution image. Now the problem is to restore a high resolution image from a sequence of low resolution, blurred, undersampled, discrete frames, where each frame has been shifted with respect to a reference frame. This problem is highly ill posed. Due to which the the solution of inverse problem may not exist, unique, or continuous or any combination of these three cases. Hence for making the solution possible we use regularized methods. Concept of regularized method is discussed widely in further chapter.

In terms of a degree of freedom(DOF) analysis we have to reconstruct an image with a higher degree of freedom equal to N^2 from undersampled degraded frames having a lower degree of freedom. The concept of the degree of freedom in an imaging system is basic to all signal processing and evolves from the desire to minimize the number of independent parameters that determine an image. Basically, the intuitive meaning of degree of freedom might be related to the concept of the number of independent samples or data points necessary to define an image. Thus, simply oversampling an image by a factor of 10 does not imply that we obtain an order of magnitude increase in degrees of freedom or independent data points, as the oversampled image pixels would have high mutual correlation. Thus, in badly blurred systems, one would expect a lower number of DOF than in a well-corrected system even though the image sampling rate remains fixed. Ideally, the DOF describing an imaging system would be an invariant measure of the maximum resolution achievable by such devices. The DOF measurement would provide a quantitative evaluation of the number of independent parameters or variables obtainable from a given system without concern to Nyquist rate and oversampling phenomena.

Hence in the multiframes superresolution problem, a higher DOF image is (re)constructed from lower DOF frames. In the recursive SR algorithm, the DOF of the reconstructed high resolution image increases after adding each new frame.

1.3 Related works

The superresolution restoration idea was first presented by Tsay and Huang [11]. They used the frequency domain approach to demonstrate the ability to reconstruct one improved resolution image from several downsampled noisefree versions of it, based on the spatial aliasing effect. In [10] single image restoration algorithm is proposed using iterative constrained least square estimation, which uses properties of a block circulant matrix; which could not be preserved for the case of undersampled frames.

Using the aliasing relationship between the undersampled frames and the reference image, a weighted recursive least square theory based algorithm is developed in the wavenumber domain [12]. They considered frames noisy and undersampled but not blurred. A frequency domain recursive algorithm for the restoration of superresolution images from noisy and blurred measurements is suggested in [13]. This algorithm could be used only

for LSI case, where the blur, the motion, and the decimation are all space variant.

The work on multi-channel superresolution has been done in [14] which is a mean of recovering high frequency information by trading off the temporal bandwidth. Since the problem is usually ill-posed, one needs to impose some regularity constraints. However, regularity constraints tend to attenuate the high frequency contents of the data (usually present in the form of discontinuities). They investigated this inherent contradiction between regularization and super-resolution issue in the context of adaptive regularization, using functions (convex, non-convex, bounded, unbounded).

Conjugate gradient methods for superresolution has been shown to accelerate convergence to the solution [15]. They utilized a combination of Tikhonov-Miller regularization and positivity constraints as a means of regularizing the conjugate gradient algorithm. R.R.Schultz and R.L.Stevenson proposed a Bayesian motion estimation technique which modeled the motion field with a discontinuity-preserving prior [16].

In [17] a unified methodology is proposed utilizing the previous image restoration tools, the maximum likelihood (ML) estimator, the maximum a posteriori probability (MAP) estimator, and the set theoretic approach using projection onto convex sets (POCS).

Michael Elad and Arie Feuer introduced the problem of reconstructing a super-resolution image sequence from a given low resolution sequence [18]. They proposed two iterative algorithms, the R-SD and the R-LMS, to generate the desired image sequence. These algorithms assumed the knowledge of the blur, the down-sampling, the sequences motion, and the measurements noise characteristics, and apply a sequential reconstruction process.

1.4 Application of Superresolution Reconstruction

Single image restoration has become a classical chapter in image processing theory, with a direct generalization to the restoration of continuous image sequences.The term *continuous* corresponds to the basic assumption that the image sequence contains one filmed scene.A standard video camera can be viewed as a source for such signals. Suppressing an additive noise in a continuous image sequence is an important preprocessing stage in many applications such as image sequence coding and computer vision algorithms. Deblurring such a signal is an important tool for the enhancement of visual data presentation to the human viewer.

In many applications such as in astronomy (satellite remote sensing) and computer vision applications, it is required to reconstruct a high-resolution image from multiframes of undersampled low resolution, blurred and noisy images. Hence the scope and application of such superresolution reconstruction methods arises in following areas.

(1) *Remote sensing:* where several images of the same area are given, and an improved resolution image is sought.

(2) *Frame freeze in video:* whereas a typical single frame in the video signal is generally of poor quality and is not suitable for hard copy printout. Enhancement of a freeze image can be effected by using several successive images merged together by a superresolution

algorithm.
(3) *Medical imaging (CT, MRI, ultrasound, etc.):* these involve the acquisition of several images, that are limited in resolution quality. In the area of quantitative autoradiography (QAR), images are obtained by exposing X-ray sensitive film to a radioactive specimen. QAR is performed in post-mortem studies, and provides a higher resolution than techniques such as positron emissiontomography (PET), X-ray computed tomography (CAT), and magnetic resonance imaging (MRI).
(4) *Conversion from NTSC video to HDTV standard:* printing from a NTSC source and conversion of NTSC source material to high definition television (HDTV) format are some recent application that motivate SR image and video reconstruction from low resolution (LR) and possibly blurred sources.

1.5 Organization of the thesis

In Chapter 1 we discuss the motivation and application of the work, different conceptions of superresolution and review the work done previously in this area. In Chapter 2, we explain the problem formulation and our algorithm. In Chapter 3, the inverse problem and its solution by least squares regularization are discussed. In Chapter 4 we discuss adaptive Wiener filtering and recursive reconstruction procedure. In Chapter 5, we discuss the results. Finally, in last in Chapter 6, we conclude the work and discuss its future potential.

Chapter 2

SR: Problem Formulation and Modelling

In this chapter, we present a new approach toward solving the superresolution problem. Simplicity and a direct connection to the problem of single image restoration (from one observed image) are the main strengths of this approach. The various known methods to restore one image from one observation are easily generalized to the new problem of single image restoration from several measured images. We start our presentation with a new model of the problem and then turn to apply known restoration methods to the suggested model. The key to a comprehensive analysis of the classical superresolution problem is to formulate the problem and to model it as simply and as efficiently as possible. We start by presenting the problem to be solved and then turn to introduce an analytical model describing it.

2.1 The Proposed Algorithm

Our algorithm is applicable to spatial domain reconstruction, in which we have considered a space varying PSF. This algorithm can be used for reconstruction from different frames obtained by multiple cameras with different sensor element sizes. The recursive reconstruction of high resolution can be started from the very first frame and adding each new frame improves the resolution of the reconstructed image. We have used different type of blurring kernels for different frames in the simulation.

After each recursion, we use our *a-priori* knowledge of the fact that each pixel value in the original image (the object) is nonnegative. Since a regularized least square solution doesn't guarantee nonnegative pixel values, we simply force all negative pixel values to zero after each recursion, thus decreasing the MSE. This given an estimate that is closer to the object and acts as a better input for the next stage of recursion. Assume that after a recursion we have an estimate $\hat{X}(m,n)$ of original image $X(m,n)$ and after making negative pixels values zero we get $\hat{X}'(m,n)$, Let MSE_1 and MSE_2 be mean square errors

before and after using the *a-priori* knowledge respectively. We can write:

$$MSE_1 = \frac{1}{L^2} \sum_{m=1}^{L} \sum_{n=1}^{L} \left[\hat{X}(m,n) - X(m,n) \right]^2 \tag{2.1}$$

where $\hat{X}(m,n)$ can take any positive or negative values.

Using a-priori knowledge we can write;

$$\hat{X}'(m,n) = \hat{X}(m,n) \quad for\ \hat{X}(m,n) \geq 0 \tag{2.2}$$

$$= 0 \quad for\ \hat{X}(m,n) < 0 \tag{2.3}$$

$$MSE_2 = \frac{1}{L^2} \sum_{m=1}^{L} \sum_{n=1}^{L} \left[\hat{X}'(m,n) - X(m,n) \right]^2 \leq MSE_1 \tag{2.4}$$

2.2 Problem Formulation

We are given N low resolution, blurred and noisy frames of different sizes $M_k \times M_k$ for $1 \leq k \leq N$. Problem is to reconstruct a high resolution image from these frames i.e. we have to find an optimal estimate of the original high resolution image.

We now present a new approach towards superresolution reconstruction. We start with the problem model and go on to find a recursive estimate of the solution. Our main emphasis shall be on how best to use the extra information obtained by adding each new frame in the recursion. There are at least two approaches to estimate the solution from the given number of constrained equations. The first approach [18] divides the given constrained equations into groups and makes an estimate by minimizing the sum of the mean square errors for each individual group.

Since the larger the number of constrained equations, the lesser is the bias on the estimate, by the above approach, the estimation error or bias for each group will be more and any estimate obtained by minimizing their sum will give a more biased result. Our approach proposes to use all the constrained equations simultaneously to estimate the solution. In our algorithm, the dimensions of $\mathbf{H}$ and $\mathbf{y}$ always increase according to the dimensions of each new frame added as shown in (4.17) and (4.18). This is the basic difference between our algorithm and that proposed in [18].

In one method, we have applied the above algorithm without any type of denoising filtering. Since a small value of λ (the regularization parameter, discussed later) gives good deblurring but poor denoising whereas a large λ provides poor deblurring but good denoising ([13] and [6]), we have taken another approach, discussed in later chapters, the two variants of which both keep λ low, and reduce the noise subsequently by subjecting the estimate to adaptive Wiener filtering [3]. The filtered estimate is used for the next recursion.

2.2.1 A Discrete Formulation of Reconstruction

We assume that an object at infinity is being imaged by N separate cameras after light from it has passed through a linear space varying medium. The medium is assumed to be locally

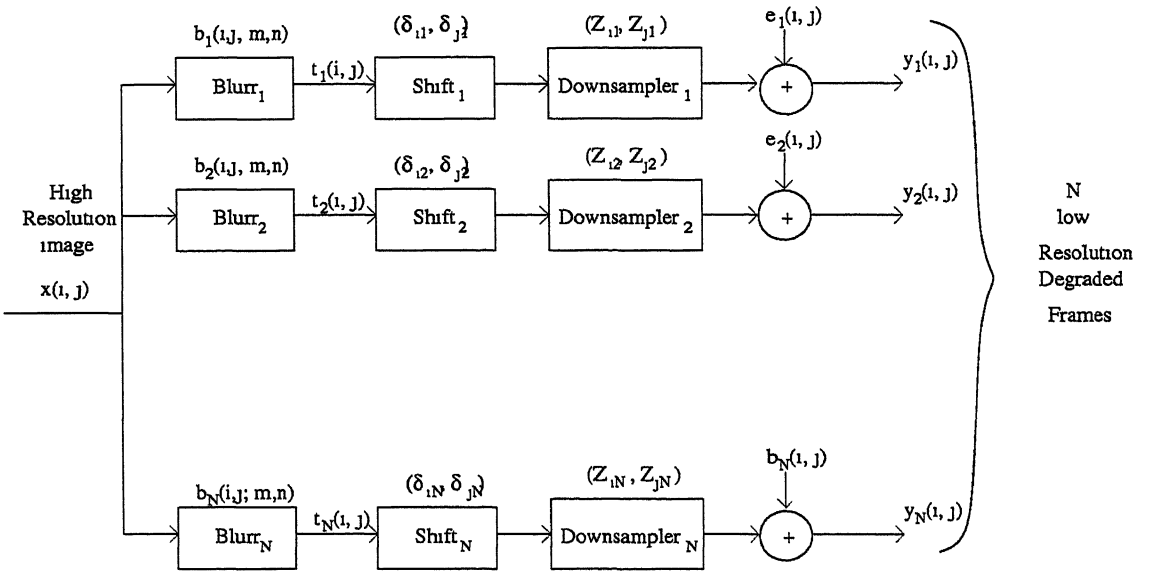

Figure 2.1: Degradation model
Figure shows the degradation model for the superresolution restoration problem

space invariant, so that each input data frame captured is blurred only by a linear space invariant PSF, even though the PSFs that blur successive frames may be different. Further, additive noise is also assumed to have been introduced.

The problem is to reconstruct a high-resolution image i.e. an estimate of the source image. Fig. 2.1 shows the overall situation of the problem under investigation. x is the object, from which we obtain N blurred 'observation' frames, These degraded frames are assumed to be obtained from the source image using the following equations: By the Fig. 2.1,

$$t_k(i,j) = \sum_{m=-\infty}^{\infty} \sum_{n=-\infty}^{\infty} b_k(i,j;m,n)\, x(m,n);\ 1 \le k \le N \tag{2.5}$$

These blurred frames are shifted by $(\delta_{i_k}, \delta_{j_k})$ and the downsampled by (Z_{i_k}, Z_{j_k}). Finally we get N degraded frames $y_k(i,j)$ by the following equations.

$$y_k(i,j) = t_k(iZ_{i_k} + \delta_{i_k}, jZ_{j_k} + \delta_{j_k}) \tag{2.6}$$

$$y_k(i,j) = \sum_{m=-\infty}^{\infty} \sum_{n=-\infty}^{\infty} b_k(iZ_{i_k} + \delta_{i_k}, jZ_{j_k} + \delta_{j_k}; m, n) * x(m,n) + e_k(i,j);\ 1 \le k \le N \tag{2.7}$$

where b_k is the blurring function for the kth frame, Z_{i_k}, Z_{j_k} are downsampling factors, and δ_{i_k}, δ_{j_k} are shifts in the i and j directions respectively, and $x(i,j)$ is the source image.

2.2.2 Vector Matrix Formulation

For Vector-Matrix notation we can rewrite, given N observation images $\{\mathbf{Y_k}\}_{k=1}^{N}$, where each image is (in the general case) of a different size $[M_k \times M_k]$. We assume that these images are different observations of the same high-resolution image $\mathbf{X}$ of size $[L \times L]$, where typically $L > M_k$ for $1 \leq k \leq N$. More specifically, each observed image is the result of a shift, a linear space-variant blurring, and uniform rational decimation performed on the ideal high-resolution image $\mathbf{X}$. We further assume that each of the observations is contaminated by nonhomogeneous additive Gaussian noise, uncorrelated across different observations. In order to treat the most general case, it is assumed that each observation is the result of different blur, noise, and decimation parameters. Translating the above description into an analytical model, we get:

Using matrix notation, we rewrite (2.7) as follows:

$$\mathbf{y_k} = \mathbf{D_k S_k B_k x} + \mathbf{e_k};\ 1 \leq \mathbf{k} \leq N \tag{2.8}$$

where $\mathbf{B_k}$ is a $[L^2 \times L^2]$ matrix representing the linear space variant blurring operator matrix, $\mathbf{S_k}$ is a $[L^2 \times L^2]$ shift operator matrix, and $\mathbf{D_k}$ is an $[M_k^2 \times L^2]$ matrix representing the decimation operator. In this model $\mathbf{y_k}$ and $\mathbf{x}$ are lexicographically ordered. $\mathbf{e_k}$ is the additive zero mean gaussian noise in the kth observation with a positive definite autocorrelation matrix $\mathbf{W_k}^{-1}$ of size $[M_k^2 \times M_k^2]$. All these matrices ($\mathbf{B_k}$,$\mathbf{S_k}$,$\mathbf{D_k}$,$\mathbf{W_k}$,$\mathbf{y_k}$) are assumed to be known. Rewriting (2.8) we get, By grouping the N equations into one from the model equations described by (2.8) we get,

$$\mathbf{y_k} = \mathbf{H_k x} + \mathbf{e} \tag{2.9}$$

where $\mathbf{H_k}$= $\mathbf{D_k S_k B_k}$. By grouping the N equations into one from the model equations described by (2.9) we get,

$$\mathbf{y} = \mathbf{H x} + \mathbf{e} \tag{2.10}$$

where
$\mathbf{y} = [\mathbf{y_1^T}\ \mathbf{y_2^T} \cdots \mathbf{y_N^T}]^\mathbf{T}$,
$\mathbf{H} = [\mathbf{H_1^T}\ \mathbf{H_2^T} \cdots \mathbf{H_N^T}]^\mathbf{T}$,
$\mathbf{e} = [\mathbf{e_1^T}\ \mathbf{e_2^T} \cdots \mathbf{e_N^T}]^\mathbf{T}$.

In solving for $\mathbf{x}$ from (2.10) which is an inconsistent linear system of equations $\mathbf{Ax} = \mathbf{b}$ where $\mathbf{A}$ is known to be an ill conditioned The least squares solution, $\mathbf{x} = \left(\mathbf{A^T A}\right)^{-1} \mathbf{A^T b}$, is not accurate enough due to ill conditioning of matrix $\mathbf{A}$. In order to obtain a stable solution, a regularization approach is used which is discussed in the next chapter.

Chapter 3

Inverse Problem and Regularization

The desire to extract information regarding the structure of a signal or image given a noise corrupted, "blurred" version of the original is a common goal in many fields of engineering and the applied sciences. These inverse problems arise in fields as diverse as geophysical exploration, medical imaging, non-destructive testing, and radar signal processing. For example, a common signal and image processing problem is that of deconvolution where one observes a filtered version of a signal in additive noise and seeks to recover the uncorrupted original.

While common enough in practice, problems such as these are notoriously difficult to solve. Most inverse problems are characterized by an unusually high sensitivity to perturbations in the data so that a small change in the measurements results in wild changes in the recovered signal.

What is an Inverse Problem?

Inverse Theory is concerned with the problem of making inferences about input data to a known system from observed output data (usually remotely sensed). Since nearly all data is subject to some uncertainty, these inferences are usually statistical. Further, since one can only record finitely many (noisy) data points and since physical systems are usually modelled by continuum equations that inherently imply bounded changes in output for bounded changes in input (at least geophysical ones are) no geophysical inverse problems are really uniquely solvable: if there is a single model that fits the data there will be an infinity of them. (A model is a parameterization of the system, usually a function.) Our goal then is to characterize the set of models that fit the data and satisfy our prejudices as well as other information.

To make these inferences quantitative one must answer three fundamental questions. How accurately are the data known? How accurately can we model the response of the system? In other words, have we included all the physics in the model that contributes significantly to the data? Finally, what is known about the problem independent of the data? This is called a priori information and is essential since for any sufficiently fine parameterization of a system there will be unreasonable models that fit the data too. Prior information is the means by which we reject or down-weight unreasonable models.

3.1 Well conditioned systems

The systems in which the mathematical problems fulfill Hadamard's definition of well-posedness for which all the following properties hold:

$$\textit{For all admissible data, a solution exists.} \tag{3.1}$$

$$\textit{For all admissible data, the solution is unique.} \tag{3.2}$$

$$\textit{The solution depends continuously on the data.} \tag{3.3}$$

are well conditioned systems.

The problems for which one or more of the above properties do not hold are ill posed problems.

If a problem is ill-posed, one is usually not too much concerned with the violation of (3.1), although of course also existence of a solution (for exact data) is an important requirement. (3.1) can usually be enforced by relaxing the notion of a solution at least for exact data, while for perturbed data, the problem has to be "regularized" and hence changed anyway.

Violation of (3.2) is considered to be much more serious. If a problem has several solutions, one either has to decide which one is of interest (e.g., the one with smallest norm, which is appropriate for some, but not all, applications) or one has to check the model for completeness and, if possible, feed in additional information. It might happen that in a practical problem, the available data (even if measured exactly at infinitely many points) simply do not determine the quantity which is sought. Then one has to "invent" additional measurements.

The question of uniqueness is relevant in inverse problems where one looks for a cause for an *observed* effect; One is usually content or even happy with having a variety of possible solutions (causes), since then, one can try to pick one which fulfills some additional criteria.

Violation of (3.3) creates serious numerical problems: if one wants to approximate a problem whose solution does not depend continuously on the data by a "traditional" numerical method as one would use for a well-posed problem, then the numerical method becomes unstable. A (partial) remedy for this is the use of "regularization methods", although one has to keep in mind that no mathematical trick can make an inherently unstable problem stable. All that a regularization method can do is to recover partial information about the solution - provide an inaccurate solution - as stably as possible. The "art" of applying regularization methods lies in finding the right compromise between accuracy and stability.

3.2 The ill conditioned nature of restoration

In the high resolution reconstruction problem where blur distortions are included, it is desirable to include the deblurring computation into the reconstruction process since the deblurring of input frames separately would introduce phase and high frequency distortions in the input frames, which is not desirable for high resolution reconstructions [13]. When the deblurring is incorporated into the high resolution restoration process, the overall reconstruction becomes unstable due to ill-conditioning of the system of equations.

The problem of image restoration is the determination of the original object distribution x given the recorded images y_k and the point spread function b. A common method of analysis of equations such as (2.7) is by operator theory. Given the space of functions that contains x and the space of functions containing the y_k, the transformation or operator T_k that maps x into y_k can be posed as

$$T_k\{x\} \longrightarrow y_k, 1 \leq k \leq N \tag{3.4}$$

where obviously for images

$$T_k\{x\} = \sum_{m=-\infty}^{\infty} \sum_{n=-\infty}^{\infty} b_k\left(iZ_{i_k} + \delta_{i_k}, jZ_{j_k} + \delta_{j_k}; m, n\right) \tag{3.5}$$

By combining all the equations for $1 \leq k \leq N$ into one from (3.4) and (3.5);

$$\mathbf{T}\{\mathbf{x}\} \longrightarrow \mathbf{y}, \tag{3.6}$$

The problem of image restoration is then to find the inverse transformation $\mathbf{T^{-1}}$ such that

$$\mathbf{T^{-1}}\{\mathbf{y}\} \longrightarrow \mathbf{x} \tag{3.7}$$

In a mathematical sense, the problem of image restoration corresponds to the existence and uniqueness of the inverse transformation. Both existence and uniqueness are important. If the inverse transformation does not exist, then there is no mathematical basis for asserting that $\mathbf{x}$ can be exactly recovered from $\mathbf{y}$. (Although there may be no mathematical basis for exactly recovering $\mathbf{x}$, there may be a practical basis for asserting that something very close to $\mathbf{x}$ can be recovered.) Problems for which there is no inverse, transformation, i.e., $\mathbf{T^{-1}}$ does not exist, are said to be singular. On the other hand , $\mathbf{T^{-1}}(\mathbf{x})$ may exist but may not be unique; i.e. $\mathbf{T^{-1}}$ may not be a function. Finally, even if $\mathbf{T^{-1}}$ exists and is unique, it may be ill-conditioned, by which we mean that a trivial perturbation in $\mathbf{y}$ can produce nontrivial perturbations in $\mathbf{x}$. That is, there exists $\mathbf{e}$, which can be made arbitrarily small such that

$$\mathbf{T^{-1}}\{\mathbf{y} + \mathbf{e}\} = \mathbf{x} + \mathbf{e}' \tag{3.8}$$

where $\mathbf{e}' >> \mathbf{e}$ is not arbitrarily small and is not negligible. Thus an ill-conditioned problem is one in which inherent data perturbations can result in undesirable effects in the solution by inverse transformation. As will be seen, image restoration problems are in this class at best and are frequently singular in addition.

3.2.1 Condition Number

Consider the elements of the matrix $\mathbf{H}$. If it is assumed that $\mathbf{H}$ is a non-trivial blur/shift/downsample operator, then it is reasonable to expect that the PSF represented by $\mathbf{H}$ is an image with considerable correlation between adjacent pixel rows and/or columns. Thus, the rows of the matrix $\mathbf{H}$ can be approximated by:

$$h(i+1,j;m,n) \cong h(i,j;m,n) + \alpha\left[h(i,j;m,n) - h(i-1,j;m,n)\right]. \tag{3.9}$$

which is to say, that in the matrix $\mathbf{H}$, index i is a row index and (3.9) shows that the $(i+1)$th row of $\mathbf{H}$ is approximately a linear combination of the ith and $(i-1)$ rows.

The relation (3.9) is of importance for the following reason: since the rows of the matrix $\mathbf{H}$ are approximately linear combinations of one another, the matrix $\mathbf{H}$ is very nearly singular. From matrix theory it is known that equations with near-singular matrices are extremely difficult to solve; i.e., they are ill-conditioned. This property of a matrix is is formally addressed in matrix theory by the *condition number*. Suppose that in the equation

$$\mathbf{y} = \mathbf{H}\mathbf{x}, \tag{3.10}$$

if the matrix $\mathbf{H}$ is a square matrix, it is known from elementary matrix theory that the rank of $\mathbf{H}$ is equal to the number of nonzero eigenvalues of $\mathbf{H}$. Let ρ_{min} and ρ_{max} be the smallest and largest eigenvalues of $\mathbf{H}$; *condition number* may be defined as

$$c(\mathbf{H}) = \left(\frac{\rho_{max}}{\rho_{min}}\right)^{1/2} \tag{3.11}$$

From (3.11) it is obvious that as $\rho_{min} \rightarrow 0$, the condition number approaches infinity. Thus, even though the matrix $\mathbf{H}$ may not be singular, near singularity is associated with very small eigenvalues and the solution of the resulting linear equations becomes difficult. In the presence of noise (whether sensor noise or computational noise) the matrix $\mathbf{H}$ can be singular within the bounds of uncertainty imposed by the noise. Solution of the digital restoration problem is thus tied to the solution of ill-conditioned (near-singular) systems of linear equations and computational methods become important.

3.2.2 In Terms of SNR

Concentrating on the former analysis, assume initially that the matrix $\mathbf{H}$ is square and nonsingular. An estimate of $\mathbf{x}$ can be generated by

$$\hat{\mathbf{x}} = \mathbf{H}^{-1}\mathbf{y}, \tag{3.12}$$

and from (2.10)

$$\hat{\mathbf{x}} = \mathbf{H}^{-1}(\mathbf{H}\mathbf{x} + \mathbf{e}) \tag{3.13}$$

$$= \mathbf{x} + \mathbf{H}^{-1}\mathbf{e}. \tag{3.14}$$

Thus, the estimate is composed of two parts: the actual object distribution and a term involving the inverse acting on the noise.

In an algebraic analysis, (2.10) is considered as a linear system with uncertainty or errors in the data; i.e., the data is "good" to a limited number of digits because of the measurement errors. If $\mathbf{H}$ has a large condition number, i.e., near singular, then the inverse $\mathbf{H}^{-1}$ will have very large entries since the determinant of $\mathbf{H}$ is small, and consequently the term $\mathbf{H}^{-1}\mathbf{e}$ will dominate the term containing the solution $\mathbf{x}$, so that in the presence of an inherent error such as $\mathbf{e}$ there is a large inherent uncertainty in the solution.

Now, assume that in (2.10)

$$\| \mathbf{y} \| = \| \mathbf{Hx} + \mathbf{e} \| \leq \| \mathbf{Hx} \| + \| \mathbf{e} \| \tag{3.15}$$

where $\| \mathbf{y} \|$ is the Euclidean norm of vector $\mathbf{y}$. Now assume that $\mathbf{H}$ preserves energy in $\mathbf{x}$; hence

$$\| \mathbf{Hx} \| = \| \mathbf{x} \|, \tag{3.16}$$

so that the relative signal-to-noise ratio (SNR) (defined in terms of norms) is

$$\frac{\| \mathbf{x} \|}{\| \mathbf{e} \|} = \alpha. \tag{3.17}$$

Now in the solution,

$$\| \hat{\mathbf{x}} \| = \| \mathbf{x} + \mathbf{H}^{-1}\mathbf{e} \| \leq \| \mathbf{x} \| + \| \mathbf{H}^{-1} \| \| \mathbf{e} \|, \tag{3.18}$$

where an Euclidean norm for both vectors and matrices is used. If the norms of the two terms in (3.18) are compared,

$$\frac{\| \mathbf{x} \|}{\| \mathbf{H}^{-1} \| \| \mathbf{e} \|} = \beta, \tag{3.19}$$

even though $\mathbf{H}$ preserves energy in $\mathbf{x}$, $\mathbf{H}^{-1}$ does not demonstrate such properties in general. Indeed, it is typical of an ill-conditioned problem that

$$\| \mathbf{H}^{-1} \| \gg 1. \tag{3.20}$$

Thus, even though the original data's signal-to-noise ratio was α, the solution possesses a signal-to-noise ratio of β and ratio of these two gives the deterioration in signal-to-noise between data and solution:

$$\begin{pmatrix} \textit{Deterioration factor in SNR} \\ \textit{from data to solution} \end{pmatrix} = \frac{\alpha}{\beta} = \| \mathbf{H}^{-1} \| . \tag{3.21}$$

For example, suppose that originally $\| \mathbf{x} \| = 100$, $\| \mathbf{e} \| = 1$, and $\| \mathbf{H}^{-1} \| = 10$. Then $\alpha = 100$, $\beta = 10$, and deterioration factor = 10. Thus, even very good signal-to-noise ratios can be deteriorated by ill-conditioning. ($\| \mathbf{H}^{-1} \| = 10$ would be considered very mild in a restoration problem; $\| \mathbf{H}^{-1} \| = 1000$ or more is typical, meaning the noise would dominate the solution for the hypothetical case posed in this example.)

3.3 Regularization

As we have seen, the equation $\mathbf{Tx} = \mathbf{y}$ is generally ill-posed when $\mathbf{T}$ is a linear operator. In particular, (2.7) is ill-posed when the kernel $h(.,.)$ is square-integrable. If we are to obtain useful approximate solutions to either of these equations, we must modify the problem in such a way that the solution becomes less sensitive to small perturbations in the data. At the same time, the solution to the modified problem must be close to the solution of the original problem. The process of modifying the original problem to achieve an acceptable compromise between these two conflicting goals is referred to as a regularization. We briefly discuss the principles of regularization in this section.

The ill-posed nature of the equation $\mathbf{Tx} = \mathbf{y}$ is a consequence not only of the nature of the operator $\mathbf{T}$ but also of the domain $D(\mathbf{T})$ over which $\mathbf{T}$ is defined. Hence, we may be able to regularize the problem at hand either by modifying $D(\mathbf{T})$ or by modifying $\mathbf{T}$ itself. Regularization involves replacing the operator $\mathbf{T}$ by an operator $\tilde{\mathbf{T}}$. Suppose further that "true" $\mathbf{y}$ is perturbed, yielding an observed signal $\tilde{\mathbf{y}}$ satisfying

$$\| \mathbf{y} - \hat{\mathbf{y}} \| \leq \varepsilon. \tag{3.22}$$

We seek a least-squares solution to the modified equation

$$\tilde{\mathbf{T}}\mathbf{x} = \tilde{\mathbf{y}}. \tag{3.23}$$

If the modified operator $\tilde{\mathbf{T}}$ has a bounded pseudoinverse $\tilde{\mathbf{T}}^{\dagger}$, the least-squares solution

$$\tilde{\mathbf{x}} = \tilde{\mathbf{T}}^{\dagger}\tilde{\mathbf{y}} \tag{3.24}$$

will be stable and is a potential candidate as an approximate solution to the original equation. We seek modifications of the original operator $\mathbf{T}$ that yield approximate solutions of the form (3.24) having an appropriate balance of accuracy and stability.

We express the original least-squares problem in the form

$$\mathbf{Tx} \simeq \tilde{\mathbf{y}}. \tag{3.25}$$

as it stands, this least-squares problem still suffers from instability and must be regularized if a useful approximate solution is to be found. A regularizer for this problem is defined as follows.

Definition: A regularizer for (3.25) is a one-parameter family of linear operators $\{\mathbf{R}_\nu, \nu \in \mathbf{A}\}$, where $\mathbf{A}$ is a set of positive real numbers with $0 \in \mathbf{A}$, satisfying

(a) For each $\nu > 0$, $\mathbf{R}_\nu$ is bounded, and

(b) $\lim_{\nu \to 0} \| \mathbf{R}_\nu \mathbf{Tx} - \mathbf{x} \| = 0$ for $\mathbf{x}$ in the range space of $T^{\dagger}$

Thus, $\mathbf{R}_\nu$ is a bounded approximation to $\mathbf{T}^{\dagger}$ and can therefore be used to obtain a stable approximate solution to (3.25) with an appropriate choice of the regularizing parameter ν.

For a given value of ν, let us take

$$\mathbf{x}_\nu = \mathbf{R}_\nu \tilde{\mathbf{y}} \tag{3.26}$$

as the approximate solution to (3.25). We then have

$$\begin{aligned} \| \mathbf{x}_\nu - \mathbf{x} \| &= \| \mathbf{R}_\nu \tilde{\mathbf{y}} - \mathbf{T}^\dagger \mathbf{y} + \mathbf{R}_\nu \mathbf{y} - \mathbf{R}_\nu \mathbf{y} \| \\ &\leq \| \mathbf{R}_\nu \tilde{\mathbf{y}} - \mathbf{R}_\nu \mathbf{y} \| + \| \mathbf{R}_\nu \mathbf{y} - \mathbf{T}^\dagger \mathbf{y} \| \\ &\leq \| \mathbf{R}_\nu \| \varepsilon + \| \mathbf{R}_\nu \mathbf{y} - \mathbf{T}^\dagger \mathbf{y} \| . \end{aligned}$$

The second term is the error due to regularization (i.e., to the fact that $\mathbf{R}_\nu$ is only an approximation to $\mathbf{T}^\dagger$), and it goes to zero as $\nu \to 0$. This term represents the effective loss of fidelity due to the application of regularization. The first term is an amplified version of the observation error. This term does not generally vanish; indeed, as $\nu \to 0$, it almost always blows up, a fact that will be established in a moment. Thus, the choice of regularizing parameter ν represents a compromise between fidelity (small regularization error) and stability (controlled noise amplification). Too large a value for ν yields a stable solution of poor fidelity, while too small a value provides insufficient regularization to overcome the ill effects of noise amplification.

Bellman [4] described the iterative approach to the solution of the ill-conditioned system of linear equations with iterative update of the regularization function. In the form of iteration, the number of equations is fixed. Therefore, no new information can be incorporated for improved solution. Under the circumstances shown in Fig.1, it is desired to get an improved solution by utilizing the additional measurements while overcoming the ill-conditioning problems. For this purpose, the application in [4] is adopted here for effective regularization, regularization information is recursively updated while new measurements are incorporated.

3.4 Least Squares Regularization for Recursive Reconstruction

In order to obtain a stable solution, a regularization approach is used which finds the solution that minimizes

$$\mathbf{R}(\mathbf{x}) = \|\mathbf{H}\mathbf{x} - \mathbf{y}\|^2 + \gamma(\mathbf{x}) \tag{3.27}$$

where $\gamma(\mathbf{x})$ is a function chosen to ensure the stability of the solution (2.10). If we know that $\mathbf{x} \approx \mathbf{c}$, then we can choose $\gamma(\mathbf{x})$ to be
$\gamma(\mathbf{x}) = \lambda\|\mathbf{x} - \mathbf{c}\|^2$ where $\lambda > 0$.
Now the overall objective functional to be minimized becomes

$$\mathbf{R}(\mathbf{x}) = \|\mathbf{H}\mathbf{x} - \mathbf{y}\|^2 + \lambda\|\mathbf{x} - \mathbf{c}\|^2 \tag{3.28}$$

and the solution $\mathbf{x}$ that minimizes $\mathbf{R}(\mathbf{x})$ is

$$\mathbf{x} = \left(\mathbf{H}^\mathbf{T}\mathbf{H} + \lambda\mathbf{I}\right)^{-1}\left(\mathbf{H}^\mathbf{T}\mathbf{y} + \lambda\mathbf{c}\right). \tag{3.29}$$

where λ is a regularization parameter (same as ν in previous section) which is adjusted to get a satisfactory compromise between stability and accuracy of the solution. λ controls the effectiveness of deblurring, high resolution reconstruction as well as noise reduction as discussed in previous section.

Chapter 4

SR: Recursive Reconstruction Procedure

In the first section of this chapter, we discuss adaptive Wiener filtering and in the second section, we present the recursive reconstruction procedure to be applied for getting a high resolution image. From (3.29), to get an estimate of $\mathbf{x}$ we must invert $\left(\mathbf{H^T H} + \lambda \mathbf{I}\right)$. Here for implementation, we have considered a small dimension image, so that the inversion in (3.29) does not take too long to compute. The computation would be quite heavy for larger dimension images. In such cases, we could use iterative methods such as the steepest descent (SD), conjugate gradient (CG) [15] etc. Bellman [4] describes an iterative approach to the solution of the ill-conditioned system of linear equations with an iterative update of the regularization function.

4.1 Adaptive Wiener Filtering

Wiener filter is a minimum mean square estimator. Let $f(n_1, n_2)$ and $q(n_1, n_2)$ be arbitrary random sequences, where $q(n_1, n_2)$ is a noisy version of $f(n_1, n_2)$ related as follows:

$$q(n_1, n_2) = f(n_1, n_2) + v(n_1, n_2) \tag{4.1}$$

it is desired to obtain an estimate, $\hat{f}(n_1,n_2)$ of $f(n_1, n_2)$ from $q(n_1, n_2)$ such that mean square error $\sigma_e^2 = E\{[f(n_1, n_2) - \hat{f}(n_1, n_2)]^2\}$ is minimized.

We use adaptive Wiener filtering because simple Wiener filtering blurs the image excessively. When an adaptive image processing method is applied to the problem of restoring an image degraded by additive random noise, it is possible to reduce background noise without significant image blurring. Two approaches to adaptive image processing have been developed. In one approach, called pixel-by-pixel processing, the processing is adapted at each pixel. At each pixel, the processing method is determined based on the local characteristics of the image, degradation, and any other relevant information in the neighbourhood region centered around the pixel. Since each pixel is processed differently, this approach is highly adaptive and does not suffer from artificial intensity discontinuities in the processed image. In another approach, called subimage-by-subimage or block-by-block processing,

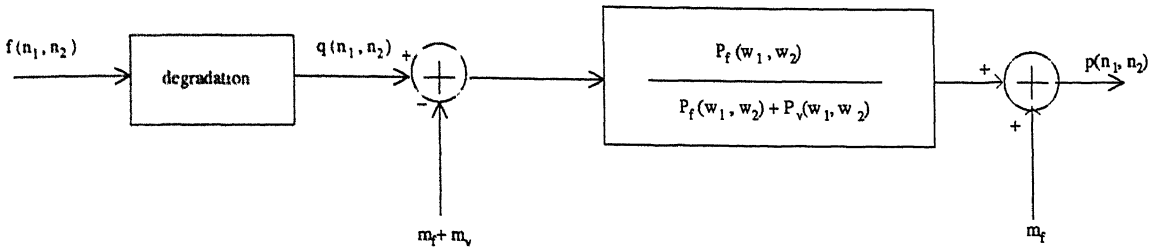

Figure 4.1: Wiener filtering
Noncausal Wiener filter for linear minimum mean square error estimation of $f(n_1, n_2)$ *from* $q(n_1, n_2) = f(n_1, n_2) + v(n_1, n_2)$.

an image is divided into many subimages, and each subimage is processed separately and then combined with the others.

Most adaptive restoration algorithms for reducing additive noise in an image can be represented by the system in Fig. 4.2. From the degraded image and prior knowledge, some measure of the local details of noise-free image is determined. One such measure is the local variance. A space variant filter $g(n_1, n_2)$ which is a function of the local image details and of additional prior knowledge is then determined.

The space-variant filter is then applied to the degraded image at the local region from which the space-variant filter was designed. When the noise is wide-band, the space-variant $g(n_1, n_2)$ is low pass in character. In low-detail image regions such as uniform intensity regions, where noise is more visible than in high details regions; a large amount (low cutoff frequency) of lowpass filtering is performed to reduce as much noise as possible. Since little signal variation is present in low detail regions, even a large amount of low pass filtering does not significantly affect the signal component. In high-detail image regions such as edges, where a large signal component is present, only a small amount of low pass filtering is performed so as not to distort (blur) the signal component. This does not reduce much noise, but the same noise is less visible in the high-detail than in the low-detail regions.

A number of different algorithms can be developed, depending on which specific measure is used to represent local image details, how the space variant $g(n_1, n_2)$ is determined as a function of the local image details, and what prior knowledge is available. One of the many possibilities is to adaptively design and implement the Wiener filter. As Fig. 4.1 shows, the Wiener filter requires knowledge of the signal mean m_f, noise mean m_v, signal power spectrum $P_f(\omega_1, \omega_2)$, and noise power spectrum $P_v(\omega_1, \omega_2)$. Instead of assuming a fixed m_f, m_v, $P_f(\omega_1, \omega_2)$ and $P_f(\omega_1, \omega_2)$ for the entire image, they can be estimated locally. This approach will result in a space-variant Wiener filter.

We first assume that the additive noise $v(n_1, n_2)$ is zero mean and white with variance of σ_v^2. Its power spectrum is $P_v\ (\omega_1, \omega_2)$ then given by

$$P_v\ (\omega_1, \omega_2) = \sigma_v^2. \tag{4.2}$$

Consider a small local region in which the signal $f(n_1, n_2)$ is assumed stationary. Within

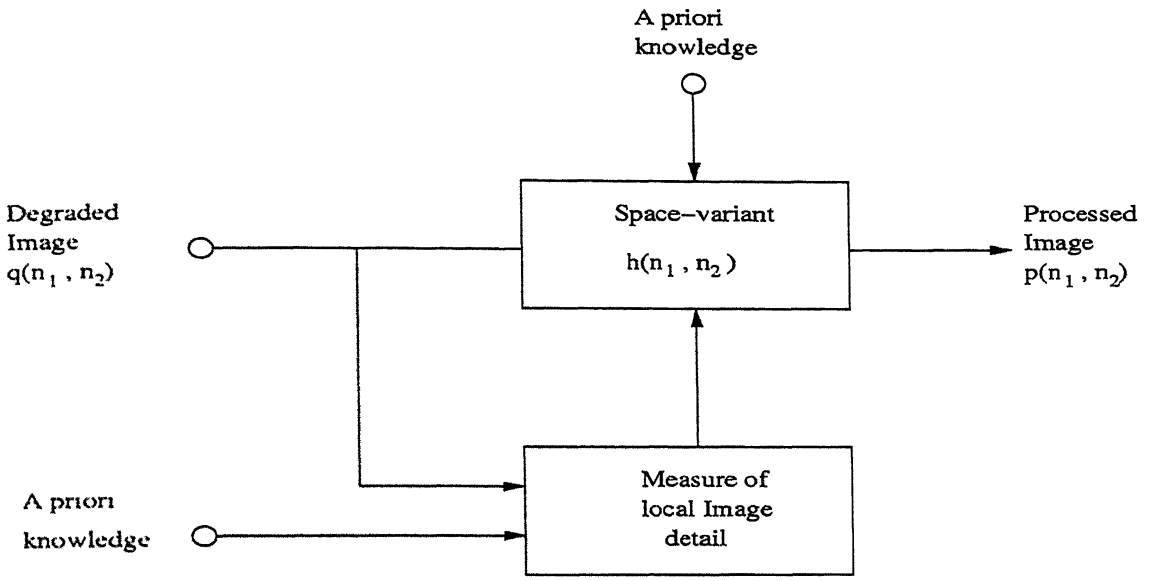

Figure 4.2: Adaptive filtering
Typical adaptive image restoration system for additive noise reduction.)

the local region, the signal $f(n_1, n_2)$ is modelled by

$$f(n_1, n_2) = m_f + \sigma_f \omega(n_1, n_2) \tag{4.3}$$

where m_f and σ_f are the local mean and standard deviation of $f(n_1, n_2)$, and $\omega(n_1, n_2)$ is zero-mean white noise with unit variance.

In (4.3), the signal $f(n_1, n_2)$ is modeled as a sum of a space-variant local mean m_f and white noise with a space-variant local variance σ_f^2. Within the local region, then, the Wiener filter $G(\omega_1, \omega_2)$ is given by

$$G(\omega_1, \omega_2) = \frac{P_f(\omega_1, \omega_2)}{P_f(\omega_1, \omega_2) + P_v(\omega_1, \omega_2)} = \frac{\sigma_f^2}{\sigma_f^2 + \sigma_v^2}. \tag{4.4}$$

from (4.4), $g(n_1, n_2)$ is a scale impulse response given by

$$g(n_1, n_2) = \frac{\sigma_f^2}{\sigma_f^2 + \sigma_v^2} \delta(n_1, n_2). \tag{4.5}$$

From (4.5) and Fig. 4.1, the processed image $p(n_1, n_2)$ within the local region can be expressed as

$$p(n_1, n_2) = m_f + (q(n_1, n_2) - m_f) * \frac{\sigma_f^2}{\sigma_f^2 + \sigma_v^2} \delta(n_1, n_2) \tag{4.6}$$

$$= m_f + \frac{\sigma_f^2}{\sigma_f^2 + \sigma_v^2} (q(n_1, n_2) - m_f) \tag{4.7}$$

If we assume that m_f and σ_f^2 are updated at each pixel,

$$p(n_1, n_2) = m_f(n_1, n_2) + \frac{\sigma_f^2(n_1, n_2)}{\sigma_f^2(n_1, n_2) + \sigma_v^2(n_1, n_2)}(q(n_1, n_2) - m_f(n_1, n_2)) \tag{4.8}$$

Noting that m_f is identical to m_q when m_v is zero (and it is indeed zero by assumption,), we can estimate $m_f(n_1, n_2)$ in (4.8) from $q(n_1, n_2)$ by

$$\tilde{m}_f(n_1, n_2) = \frac{1}{(2M+1)^2} \sum_{k_1=n_1-M}^{n_1+M} \sum_{k_2=n_2-M}^{n_2+M} q(k_1, k_2) \tag{4.9}$$

where $(2M+1)^2$ is the number of pixels in the local region used in the estimation.

Since $\sigma_q^2 = \sigma_f^2 + \sigma_v^2$, σ_f^2 may be estimated from $g(n_1, n_2)$ by

$$\hat{\sigma}_f^2(n_1, n_2) = \begin{cases} \hat{\sigma}_q^2(n_1, n_2) - \sigma_v^2, & if\ \hat{\sigma}_q^2(n_1, n_2) > \sigma_v^2 \\ 0 & otherwise \end{cases} \tag{4.10}$$

where

$$\hat{\sigma}_q(n_1, n_2) = \frac{1}{(2M+1)^2} \sum_{k_1=n_1-M}^{n_1+M} \sum_{k_1=n_2-M}^{n_2+M} (q(k_1, k_2) - \hat{m}_f(n_1, n_2))^2 . \tag{4.11}$$

4.2 Recursive Reconstruction Procedure

In this section we show how to make recursive the procedure to update the estimate. Since the solution given by (3.29) does not guarantee a reconstruction with nonnegative pixel values, we use the a-priori information that $\mathbf{x}(i) \geq 0$ *for* $1 \leq i \leq L^2$, and, after each recursion, set all negative pixel values to zero thereby decreasing the MSE. This obviously gives an estimate that is closer to the desired one and acts as a better input for the next stage of recursion. The Wiener filter output for the estimate $\mathbf{x_k}$ is denoted by $\mathbf{w_k}$.

Initialization : λ=0.01.

$$\mathbf{c}(\mathbf{1}) = \mathbf{0}; \tag{4.12}$$

$$\mathbf{H}'(\mathbf{1}) = \mathbf{H_1}; \tag{4.13}$$

$$\mathbf{y}'(\mathbf{1}) = \mathbf{y_1}; \tag{4.14}$$

$$\mathbf{x_1} = \left(\mathbf{H}'(\mathbf{1})^{\mathbf{T}} \mathbf{H}'(\mathbf{1}) + \lambda \mathbf{I}\right)^{-1} \left(\mathbf{H}'(\mathbf{1})^{\mathbf{T}} \mathbf{y}'(\mathbf{1}) + \lambda \mathbf{c}(\mathbf{1})\right). \tag{4.15}$$

Update: $1 \leq k \leq 16$

$$\mathbf{c}(\mathbf{k}) = \mathbf{w_{k-1}}; \tag{4.16}$$

$$\mathbf{H}'(\mathbf{k}) = \left[\mathbf{H}'^{\mathbf{T}}(\mathbf{k-1}) \quad \mathbf{H_k^T}\right]^{\mathbf{T}}; \tag{4.17}$$

$$\mathbf{y}'(\mathbf{k}) = \left[\mathbf{y}'^{\mathbf{T}}(\mathbf{k-1}) \quad \mathbf{y_k^T}\right]^{\mathbf{T}}; \tag{4.18}$$

$$\mathbf{x_k} = \left(\mathbf{H}'(\mathbf{k})^{\mathbf{T}} \mathbf{H}'(\mathbf{k}) + \lambda \mathbf{I}\right)^{-1} \left(\mathbf{H}'^{\mathbf{T}}(\mathbf{k}) \mathbf{y}'(\mathbf{k}) + \lambda \mathbf{c}(\mathbf{k})\right). \tag{4.19}$$

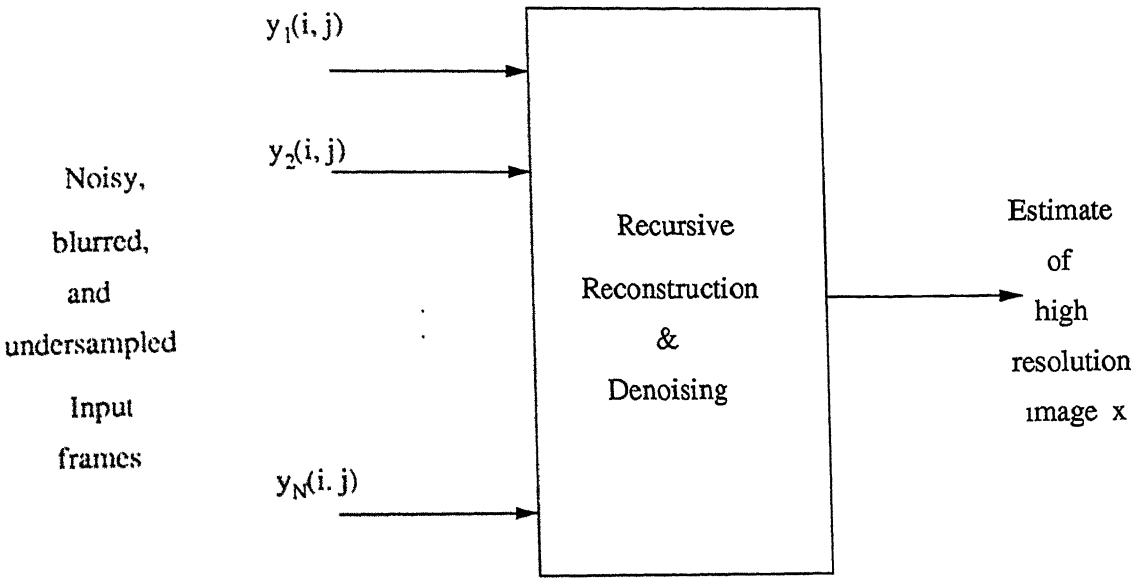

Figure 4.3: Recursive reconstruction
Recursive reconstruction model for a high resolution image from N degraded undersampled frames.

In the next chapter, we discuss the implementation and compare the results obtained by different algorithms.

Chapter 5

Implementation and Discussion

In this chapter we discuss about two algorithm. First one is for reconstruction of a high resolution image from several degraded frames, which is much computationally expensive. Second algorithm is for reconstruction of a high resolution image from a degraded frame blurred by a separable point spread function.

5.1 First Algorithm: Computer Simulation and Results

For simulation on MATLAB we use 'cameraman.tif' image of size 32×32. The reason for taking a small image is to lessen the simulation run time. From this picture we obtain 16 undersampled, blurred and noisy frames of size 8×8. The blurring kernel $\mathbf{H_k}$; $1 \leq k \leq 16$ for each frame is different.

Hence the computer simulations use 16 frames of 8×8 noisy, blurred and undersampled images as the input frames in order to reconstruct 32×32 high resolution image. The low resolution blurred input frames are obtained as follows. First 32×32 original image is blurred by different types of 2-D Atmospheric turbulence blur and Motion blur. Then the image is downsampled with various sampling references to get low-resolution frames with different shifts. Then Gaussian distributed noise are added in each frame. Fig. shows the 16 input frames of size 8×8. For simulation we have taken the value of regularization parameter λ as 0.01.

We show the improvement in the estimated image after adding each new frame both by visual comparison and by plotting the mean square error.

We compare the results from our algorithm with those obtained by [18] on the basis of mean square error of the estimate. We have given equal weight to each past frame: the use of a weighted least squares approach and/or a smoothing operator [18] might improve the results further.

For purposes of comparison, we consider various different cases as follows:

Case 1. SR images obtained without Wiener filtering of the estimate obtained from (4.19): then (4.16) becomes $\mathbf{c}(\mathbf{k}) = \mathbf{x_{k-1}}$.

Case 2. SR images obtained using (4.16) to (4.19). But now, Wiener filtering is applied only to prepare the input data for the next recursion, while the partially re-solved image after the kth recursion is taken to be $\mathbf{x_k}$.

Case 3. SR images obtained using (4.16) to (4.19). This means Wiener filtering is applied to prepare the input data for the next recursion, and the partially resolved image after the kth recursion is taken to be $\mathbf{w_k}$.

Case 4. SR image obtained by method suggested in [13].

Case 5. SR images obtained by using the recursive algorithm given in [18].

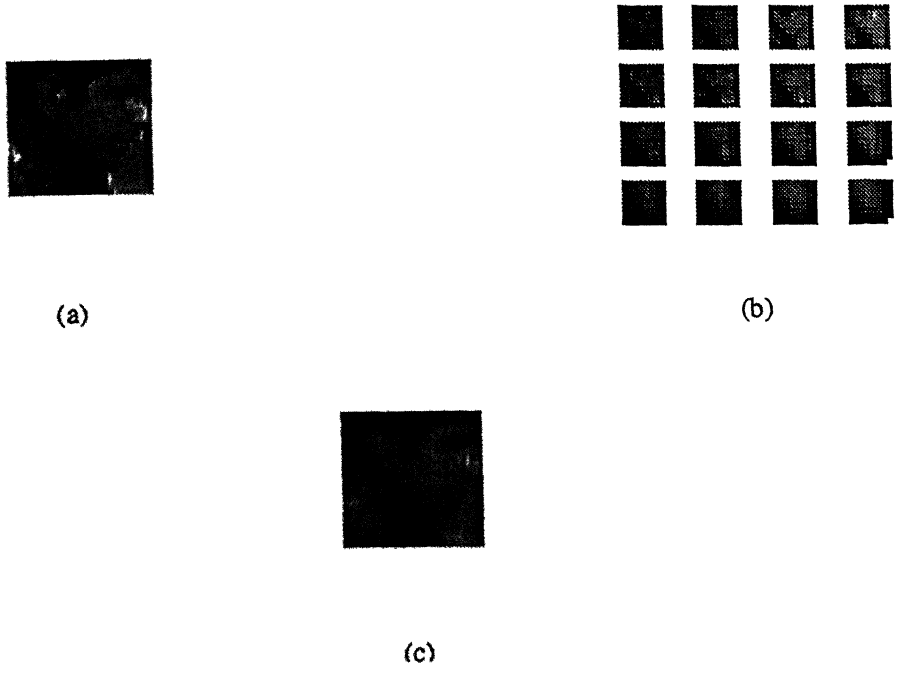

Figure 5.1: (a) Original image of sizes 32 × 32, (b) Input degraded frames of sizes 8 × 8, (c) Reconstructed image according to case4.

In results we have discussed two observations. In first one the reconstruction of high resolution image is started from the first frame. In second observation we have started reconstruction assuming six frames available.

Fig. 5.1 is common for both the two observations. Fig. 5.1(a) shows the original image of size 32 × 32. Fig. 5.1(b) shows the input undersampled, blurred and noisy frames of size 8 × 8. Fig. 5.1(c) shows the constructed image described as in case4.

5.1.1 First Observation: Computer Simulation and Results

The result for case4 is same irrespective of input MSEs order. Now we discuss about the observation when the MSEs of the input frames are in random fashion. Case2 is still best

on the bases of comparing the MSE among all the cases. But the output in case2 is some blurred due to single time denoising by the Wiener filtering in each recursion.

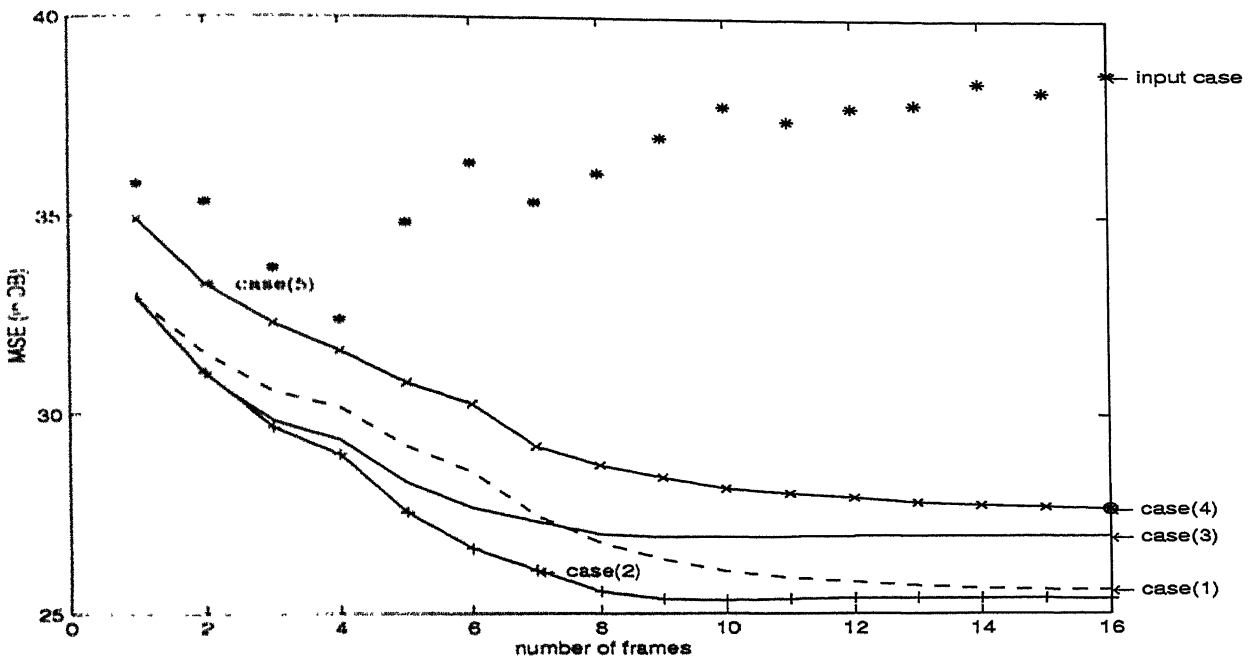

Figure 5.2: Random ordered Input MSE: MSE comparisons graph for different cases.

5.1.2 Second Observation: Computer Simulation and Results

Here we discuss about second observation. It is observed that if the recursion is commenced, not from frame k = 1, but at a frame k_0 further down, and the proposed algorithm (case2) is modified as described below, the MSE at k = 16 is lower than that seen when the same algorithm is applied from k = 1.

Initialization: λ=0.01.

$$\mathbf{c}(\mathbf{k_0}) = \mathbf{0}; \tag{5.1}$$

$$\mathbf{H'}(\mathbf{k_0}) = \left[\mathbf{H_1^T}\ \ \mathbf{H_2^T} \cdots \mathbf{H_{k_0}^T}\right]^{\mathbf{T}}; \tag{5.2}$$

$$\mathbf{y'}(\mathbf{k_0}) = \left[\mathbf{y_1^T}\ \mathbf{y_1^T} \cdots \mathbf{y_{k_0}^T}\right]^{\mathbf{T}}; \tag{5.3}$$

$$\mathbf{x_{k0}} = \left(\mathbf{H'}(\mathbf{k_0})^{\mathbf{T}}\mathbf{H'}(\mathbf{k_0}) + \lambda\mathbf{I}\right)^{-1}\left(\mathbf{H'}(\mathbf{k_0})^{\mathbf{T}}\mathbf{y'}(\mathbf{k_0}) + \lambda\mathbf{c}(\mathbf{k_0})\right). \tag{5.4}$$

Update: $\mathbf{k_0 < k \leq 16}$

$$\mathbf{c}(\mathbf{k}) = \mathbf{w_{k-1}}; \tag{5.5}$$

$$\mathbf{H}'(\mathbf{k}) = \left[\mathbf{H}'(\mathbf{k}-\mathbf{1})^{\mathbf{T}} \quad \mathbf{H}_{\mathbf{k}}^{\mathbf{T}}\right]^{\mathbf{T}}; \tag{5.6}$$

$$\mathbf{y}'(\mathbf{k}) = \left[\mathbf{y}'(\mathbf{k}-\mathbf{1})^{\mathbf{T}} \quad \mathbf{y}_{\mathbf{k}}^{\mathbf{T}}\right]^{\mathbf{T}}; \tag{5.7}$$

$$\mathbf{x_k} = \left(\mathbf{H}'(\mathbf{k})^{\mathbf{T}}\mathbf{H}'(\mathbf{k}) + \lambda\mathbf{I}\right)^{-1}\left(\mathbf{H}'(\mathbf{k})^{\mathbf{T}}\mathbf{y}'(\mathbf{k}) + \lambda\mathbf{c}(\mathbf{k})\right). \tag{5.8}$$

This is demonstrated in Fig. 5.4 and Fig. 5.5 for a starting frame of k = 6. The reason for this phenomenon is not conclusively evident, but it is likely that, after adding a certain number of frames, noise amplification starts in the partially resolved SR image [13] and this noise propagates through the recursion, The curve for case2 in Fig. 5.2 after k = 10 supports this hypothesis.

At present, further study of this phenomenon is required before a clear picture emerges, and questions such as whether there exists an 'optimal' start frame number, can be answered.

5.2 Second Algorithm: Computer Simulation and Results

Now further we discuss about a new computationally efficient method for separable PSF taking the fact that 2-D shift matrix and 2-D downsampling matrix are always separable and for getting a stable and unique solution of the ill-conditioned equations we use empirical regularized least square method. The direct inversion of $\left(\mathbf{H}^{\mathbf{T}}\mathbf{H} + \lambda\mathbf{I}\right)$ raises several difficulties which render the solution of (3.29) impractical. The main one is the computational burden required here. In a typical video application the size of the matrix is $L^2 \times L^2$ (e.g. for L=1000), we will be required to invert a $10^6 \times 10^6$ matrix). Since computational complexity for finding the inverse of a matrix of size $[N \times N]$ is of N^3 order. Eq. (3.29) is having matrix of size $[L^2 \times L^2]$, which will have computational complexity of L^6 order. For overcoming such situation, in the proposed algorithm we have exploited the separable property of shift matrix $\mathbf{S}$ and downsample matrix $\mathbf{D}$, hence if the blurring matrix $\mathbf{B}$ is also separable according to following equations

$\mathbf{D} = \mathbf{D_1} \otimes \mathbf{D_2}$

$\mathbf{S} = \mathbf{S_1} \otimes \mathbf{S_2}$

$\mathbf{B} = \mathbf{B_1} \otimes \mathbf{B_2}$

Using above relations rewriting (2.8),

$$\mathbf{Y} = \mathbf{D_1}\mathbf{S_1}\mathbf{B_1}\mathbf{X}\mathbf{B_2}\mathbf{S_2}\mathbf{D_2} + \mathbf{E} \tag{5.9}$$

where each entity in above equation is a matrix. $\mathbf{B_1}, \mathbf{B_2}, \mathbf{S_1}$ and $\mathbf{S_2}$ each is of size $[L \times L]$ and $\mathbf{D_1}, \mathbf{D_2^T}$ are of size $[M \times L]$ and $\mathbf{Y}, \mathbf{E}$ are of size $[M \times M]$. Rewriting (5.9) we get,

$$\mathbf{Y} = \mathbf{H_1}\mathbf{X}\mathbf{H_2} + \mathbf{E} \tag{5.10}$$

where $\mathbf{H_1} = \mathbf{D_1}\mathbf{S_1}\mathbf{B_1}$ and $\mathbf{H_2} = \mathbf{D_2}\mathbf{S_2}\mathbf{B_2}$. If we use regularized least square method for getting estimate of $\mathbf{X}$ from (5.10), we get the same estimate equation as (3.29), due to which

our motive of considering PSF to be separable seems useless. Hence for making solution possible and computationally efficient, we propose an empirical formula for separable case, which is inspired by (3.29).

From $\mathbf{H} = \mathbf{H}_1 \otimes \mathbf{H}_2$ for getting empirical solution, a partial estimate $\mathbf{X}_1$ of $\mathbf{X}$ can be given as follows considering only $\mathbf{H}_1$,

$$\mathbf{X}_1 = \left(\mathbf{H}_1^{\mathrm{T}}\mathbf{H}_1 + \lambda\mathbf{I}\right)^{-1}\left(\mathbf{H}_1^{\mathrm{T}}\mathbf{Y}\right), \tag{5.11}$$

similarly for considering only $\mathbf{H}_2$ another partial estimate $\mathbf{X}_2$ of $\mathbf{X}$ can be given as follows

$$\mathbf{X}_2 = \left(\mathbf{Y}\mathbf{H}_2^{\mathrm{T}}\right)\left(\mathbf{H}_2^{\mathrm{T}}\mathbf{H}_2 + \lambda\mathbf{I}\right)^{-1}, \tag{5.12}$$

Now considering both $\mathbf{H}_1$ and $\mathbf{H}_2$ simultaneously and combining above both partial estimates, we can write a empirical estimate of source image as follows:

$$\mathbf{X} = \left(\mathbf{H}_1^{\mathrm{T}}\mathbf{H}_1 + \lambda\mathbf{I}\right)^{-1}\left(\mathbf{H}_1^{\mathrm{T}}\mathbf{Y}\mathbf{H}_2^{\mathrm{T}}\right)\left(\mathbf{H}_2^{\mathrm{T}}\mathbf{H}_2 + \lambda\mathbf{I}\right)^{-1} \tag{5.13}$$

Now for obtaining estimate from (5.13), we have to invert two matrices each of size $L \times L$. That is easily practically implementable.

In next section we will compare the results obtained by actual regularized least square method and proposed empirical least square regularized method.

In this section we have compared the results of the proposed algorithm with two different cases. In first case the estimate of the high resolution image is found by interpolation, deshifting, deblurring and further denoising by Wiener filtering or median filtering. In the second case the estimate of the original image is found by actual regularized least square method given in (3.29), which is quite computationally expensive.

For simulation on MATLAB we use 'cameraman.tif'. We have taken the size of image as 256×256 for comparison with first case and 32×32 for comparison with second case. For getting degraded frame first we blur the original image by 2-D motion blurring, then shift it (here for simulation we have taken zero shift in both directions.), then downsample it by 2 and finally add white Gaussian noise. We compare the estimate of the first case with the estimate of the proposed algorithm for two different values of noise variance[$\sigma^2 = 0.001$ and $\sigma = 0.01$]. The estimate by the first case deteriorates very fast with the increasing noise variance which is also clear from Fig. 5.6c, Fig.5.6d, and Fig. 5.7b. While the estimate by proposed algorithm remains consistent as shown in Fig. 5.6e and Fig. 5.7c.

For second comparison we use image of size 32 × 32. The reason for taking small size is computations in second case. By Fig. 5.8 it is clear that the proposed algorithm is equally good as case second with drastic change in computational time.

The simulation run time for 32 × 32 image is more than 30 minutes by (3.29) and restoration of same image by (5.13) takes few seconds. When the image of size 256 × 256 is restored by (5.13), the simulation run time is even less than 1 minute. which is really remarkable. The restoration of the same image by (3.29) is unimaginable.

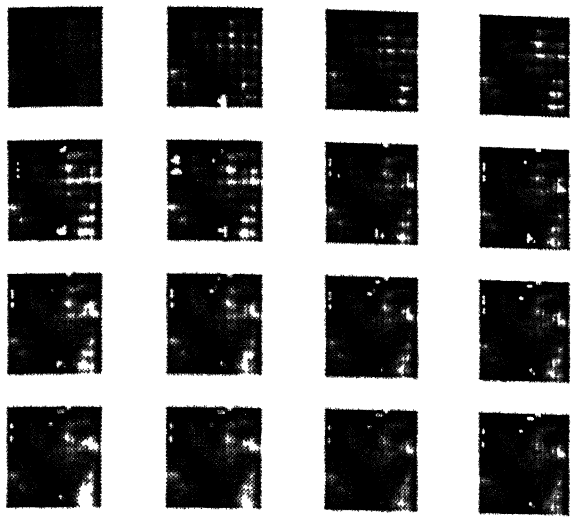

(a)

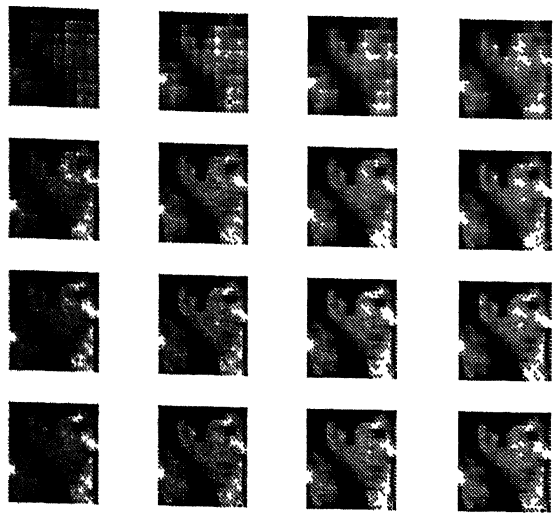

(b)

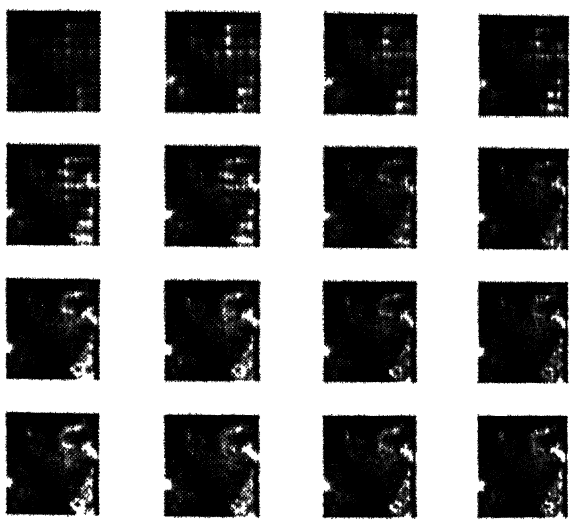

(c)

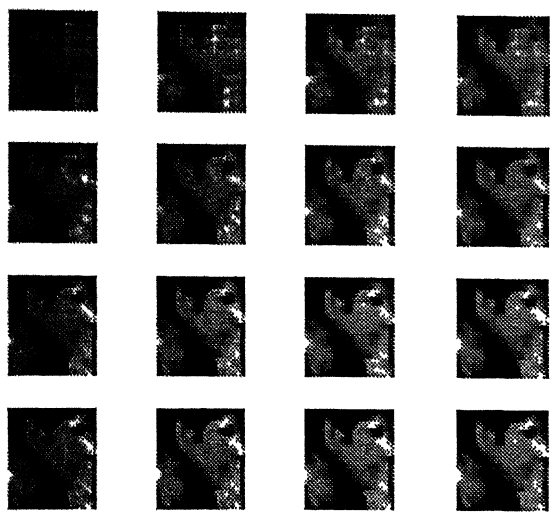

(d)

Figure 5.3: Random ordered Input MSE: (a) Reconstructed image according to case5, (b) Reconstructed image according to case2, (c) Reconstructed image according to case1, (d) Reconstructed image according to case3.

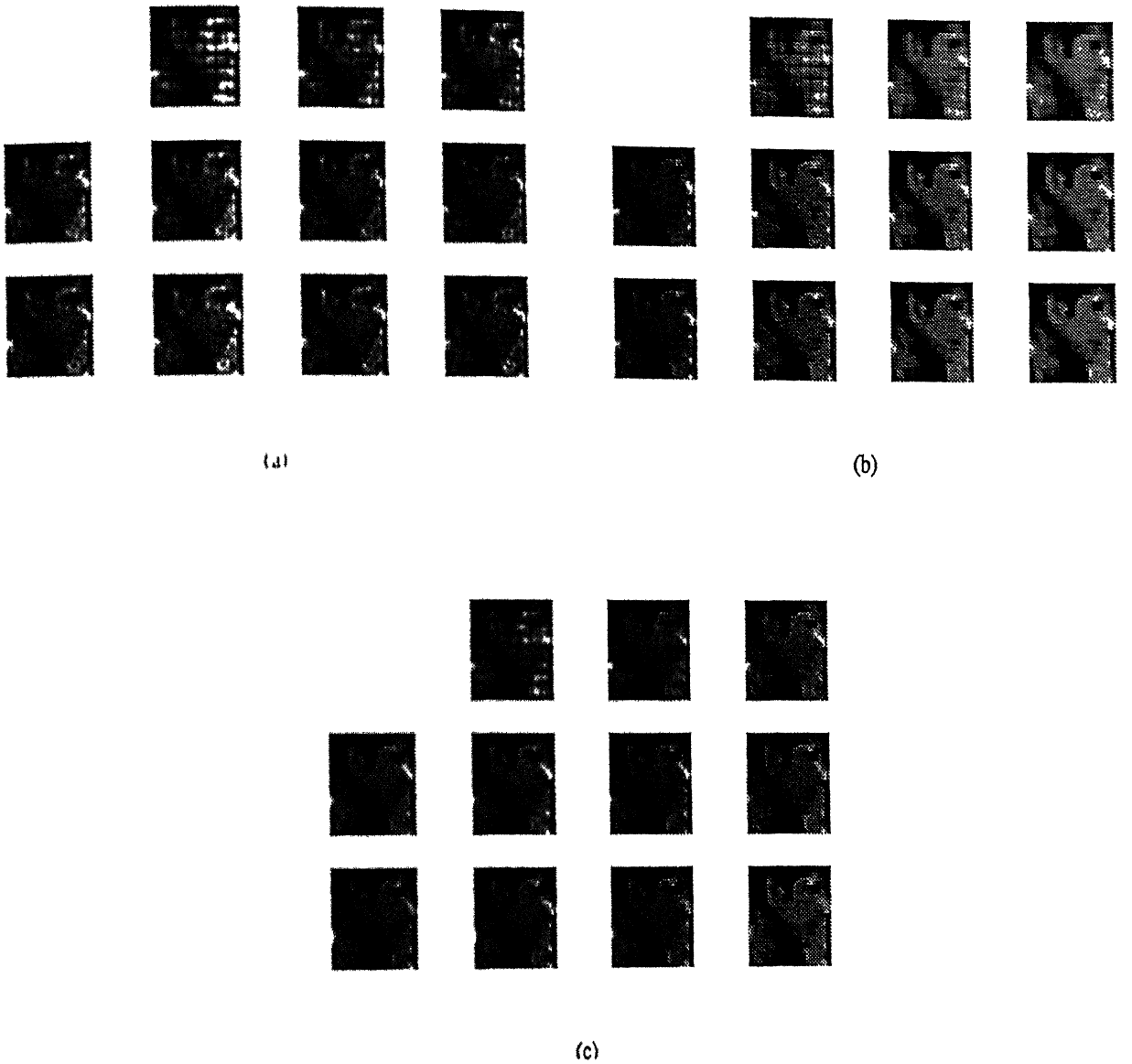

Figure 5.4: Recursive reconstruction: (a) Reconstructed image according to case1, (b) Reconstructed image according to case2, (c) Reconstructed image according to case3.

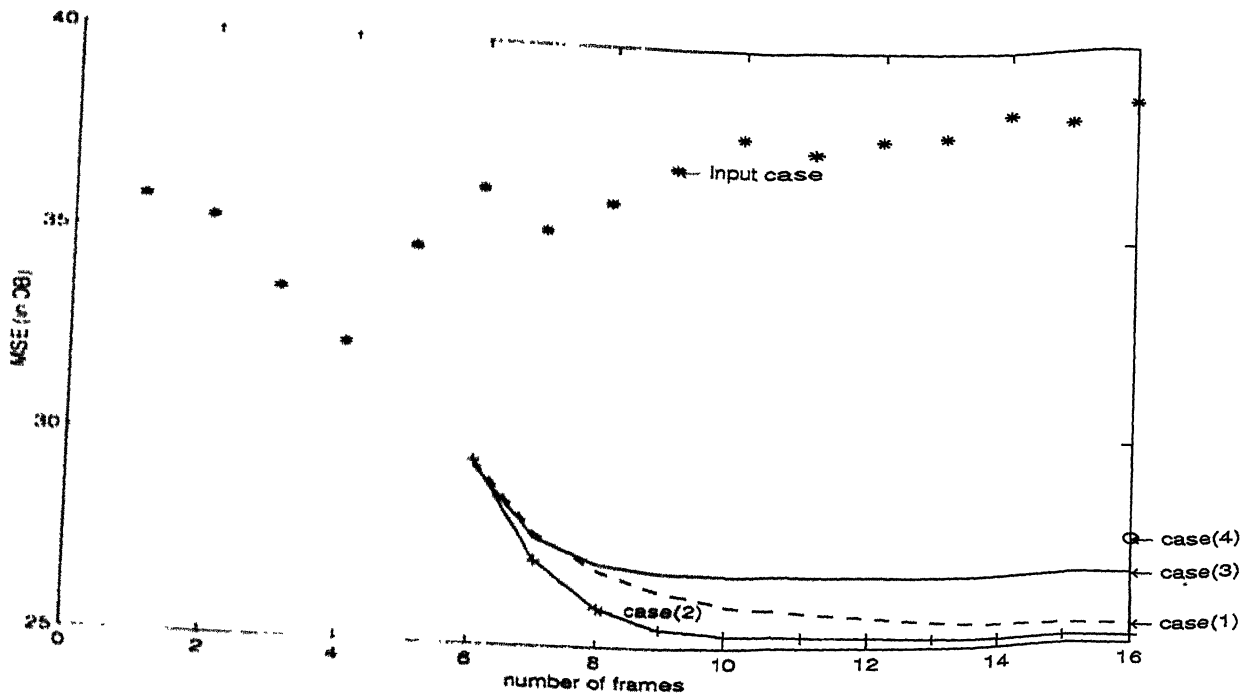

Figure 5.5: Recursive reconstruction : MSE comparisons graph for different cases.

(a)

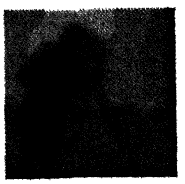

(b)

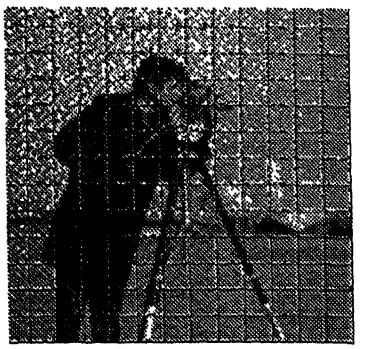

(c)

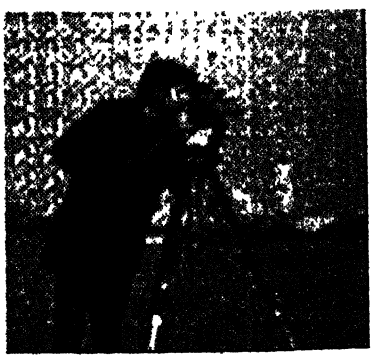

(d)

(e)

Figure 5.6: (a) Original image of size 256 × 256, (b) Input frame of size 128 × 128 with noise variance σ^2=0.001 , (c) Wiener filtered reconstructed image for first case, (d) Median filtered reconstructed image for first case, (e) Reconstruction according to proposed algorithm .

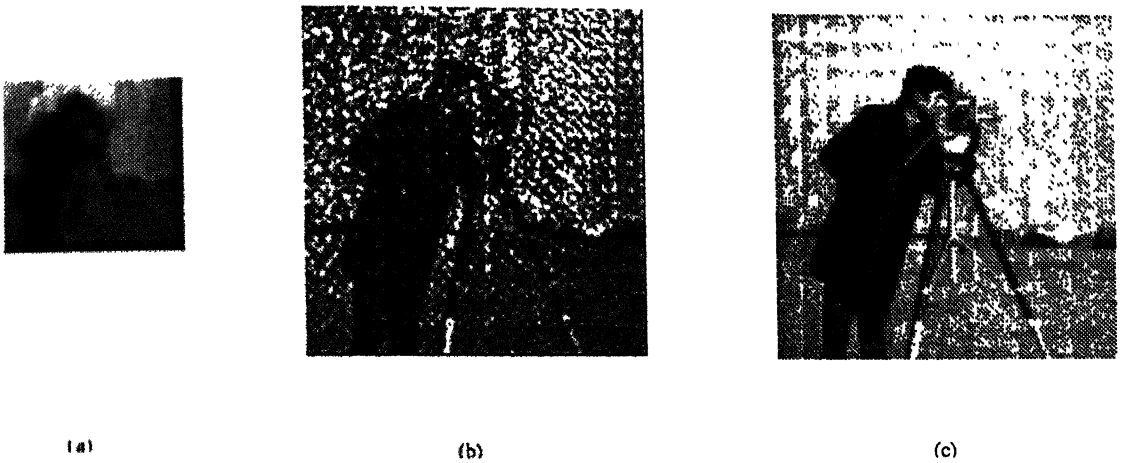

(a) (b) (c)

Figure 5.7: (a) Input frame of size 128 × 128 with noise variance σ^2=0.01, (b) Median filtered reconstructed image for first case, (c) Reconstruction according to proposed algorithm

.

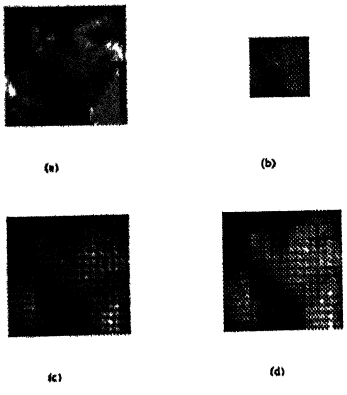

(a) (b)

(c) (d)

Figure 5.8: Comparison in second case and proposed algorithm:(a) Original image of size 32 × 32, (b) Input degraded frame of size 16 × 16, (c) Estimated image by eq. (3.29) (d) Estimated image by eq. (5.13)

Chapter 6

Conclusion

In this chapter we conclude the thesis and discuss about the future work which can be proceeded further.

The proposed first algorithm gives better results but its computational complexity is substantial. This can perhaps be reduced by using some iterative methods such as SD and CG etc. The LMS algorithm for fast reconstruction given in [18] will give better results if we use our proposed recursive algorithm. In the second proposed algorithm we have restored an image from a single degraded frame blurred by separable point spread function which is very much computationally efficient.

6.1 Future work

As discussed in chapter5, if we start recursion from other frame but not the first frame, the optimum start frame has to be find out by keeping compromise between deblurring and denoising in the final reconstructed SR image. Second work can be extended to get a high resolution image from several degraded, undersampled frames for separable point spread function which would be a good achievement as computational complexity point of view for applications in astronomy.

References

[1] A.K. Jain, *Fundamentals in Digital Image Processing.* Englewood cliffs, NJ; Prentice-Hall, 1989.

[2] H.C. Andrews and B.R. Hunt, *Digital Image Restoration.* Englewood cliffs, NJ; Prentice-Hall, 1977.

[3] Jae S. Lim and Joe S. Lim, *2D Signal and Image Processing.* Prentice Hall, 1990.

[4] Richard Bellman, *Introduction to Matrix Analysis.* 2nd edition New York:McGraw-Hill, 1970

[5] Heinz W.Engl, Martin Hanke and Andreas Neubauer, *Regularization of Inverse Problems.* Kluwer Academic Publishers, 2000.

[6] Henry Stark, *Image Recovery: Theory and Application.* Academic Press, Inc., Orlando, Florida, 1987.

[7] Mark R. Banham and Aggelos K. Katsaggelos,"Digital Image Restoration," *IEEE Signal Processing Magazine,*pp. 24-41, March 1997.

[8] K. S. Sisodia, K. S. Venkatesh, and Sumana Gupta, "Spatial Domain Superresolution Reconstruction from Several Degraded Frames," *Submitted in ICIP-2001, Greece.*

[9] K. S. Sisodia, K. S. Venkatesh, and Sumana Gupta, "Spatial Domain Image restoration from a Noisy, Undersampled Frame, Blurred by a Separable Point Spread Function.," *Submitted in SPCOM-01, Banglore.*

[10] B.R. Hunt, "The application of constrained least squares estimation to image restoration by digital computer," *IEEE Trans. on Computers,* Vol. C-22, No. 9, September 1973.

[11] T.S. Huang and R.Y. Tsay, "Multiple frames image restoration and registration," in *advances in Computer Vision and Image Processing,* vol.1, pp. 317-339, 1984.

[12] S.P. Kim, N.K. Bose, and H.M. Valenzuzuela, "Recursive recostruction of high resolution image from noisy undersampled multiframes," *IEEE Trans. ASSP, vol.38, pp. 1013-1027, June 1990.*

[13] S.P. Kim, and Wen-Yu-Su, "Recursive high-resolution reconstruction Of blurred multiframe image," *IEEE Transaction on Image processing,* Vol.2, No.4, pp 534-539, Oct.1993.

[14] A. Lorette, H. Shekarforoush and J. Zerubia, "Super-resolution with adaptive regularization," *ICIP Proceedings,* vol.1, 1997.

[15] T.J. Connolly and R.G. Lane, "Gradient methods for superresolution," *ICIP* vol.1, 1997.

[16] R.R. Schultz and R.L. Stevenson, "Bayesian estimation of subpixel resolution motion fields and high resolution video stills," *ICIP*, vol.3, 1997.

[17] Michael Elad and Arie Feuer, "Restoration of a Single Superresolution Image from Several Blurred, Noisy and Undersampled Measured Images," *IEEE Trans. Image Processing*, No. 6, pp. 1646-1658, Dec. 1997.

[18] Michael Elad and Arie Feuer, "Superresolution Restoration of an Image Sequence: Adaptive Filtering Approach," *IEEE Trans. on Image Processing,* Vol. 8, No. 3, March 1999.